

TWO-COLOR MULTIPHOTON DISSOCIATION/IONIZATION OF JET-COOLED $\text{Cr}^{\text{III}}(\text{acac})_3$ AND $\text{Cr}^0(\text{CO})_6$. APPEARANCE ENERGIES OF Cr ATOM

Naohiko MIKAMI, Rie OHKI and Hiroaki KIDO

Department of Chemistry, Faculty of Science, Tohoku University, Sendai 980, Japan

Received 16 May 1988; in final form 8 August 1988

Photodissociation of jet-cooled $\text{Cr}^{\text{III}}(\text{acac})_3$ and $\text{Cr}^0(\text{CO})_6$ has been investigated by two-color multiphoton dissociation/ionization spectroscopy in which a UV light of 258–242 nm is used for the dissociation and a visible light for the multiphoton ionization of photofragments. The generation of the neutral Cr atom is found in both compounds after two-photon excitation with the UV light. The threshold energies of the two-photon dissociation are determined and the characteristic fragmentations are observed. For $\text{Cr}^{\text{III}}(\text{acac})_3$ it is found that no fragment other than the Cr atom is produced by the two-photon dissociation and that the threshold energy for Cr atom generation is about 78500 cm^{-1} (9.73 eV). The result suggests that the neutral Cr atom originates directly from the super-excited state which is the neutral excited state lying at about 2.27 eV higher than the ionization potential of $\text{Cr}^{\text{III}}(\text{acac})_3$. For $\text{Cr}^0(\text{CO})_6$, the production of the coordinatively unsaturated photofragments is found in the photodissociation with the UV light and the sequential mechanism for the Cr atom generation is confirmed.

1. Introduction

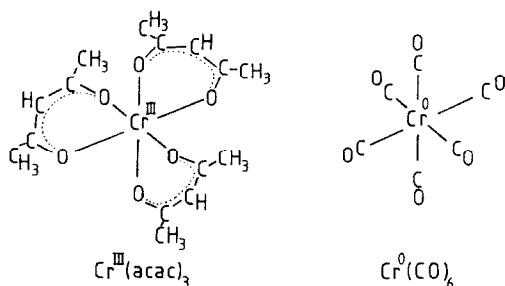
Gas phase photochemistry of transition metal coordination compounds has been the focus of recent laser spectroscopic investigations [1]. One of interesting features in the gas phase photodissociation of these compounds is the generation of free metal atoms, which was first observed by Callear and Oldman in flash photolysis of iron pentacarbonyl [2,3]. In recent studies the metal atom generation has been investigated by laser photolysis with high intensity lasers which often involves multiphoton dissociation (MPD). Resonance enhanced multiphoton ionization (MPI) is frequently used as a sensitive detection method of the metal atom, so that multiphoton dissociation/ionization (MPD/MPI) has been popular in those studies [4–12]. The chromium carbonyls are among well-studied systems by the MPD/MPI method [10–16]. It has been shown that the dissociation to Cr and CO is extremely efficient compared with the competing ionization of the parent compounds [10–12]. The efficient fragmentation producing the coordinatively unsaturated compounds has also been investigated by transient infrared spec-

troscopy with excimer laser photolysis [17–23]. In spite of such an efficient dissociation, the dissociation energy required in removing all of the CO ligands has not yet been determined. In MPD/MPI experiments, the laser power dependence of the Cr^+ ion yield represents a key factor in the determination of the dissociation energy. Although large indices (more than six) have often been found in the power dependence of the MPD/MPI process [12,14], the multiphoton energy determined by the observed index is not adequate for estimation of the dissociation energy, as pointed out by Fisanick et al. [12]. They emphasized that a simple rate equation model for the analysis of the MPD/MPI processes failed because of a coherent interaction between molecules and radiation field under an intense photon flux. In addition to this complication, both multiphoton processes proceed simultaneously under a high-intensity radiation field of a single laser, as far as the one-color MPD/MPI method is employed. This method involves two different generation processes of the metal ion; one is the photodissociation of the photoionized compounds and the other is the photoionization after the photodis-

sociation. Thus, the energetics of the dissociation mechanism become rather complicated.

In the present work we report a photodissociation study of the Cr atom generation of jet-cooled chromium coordination compounds in the gas phase using the two-color MPD/MPI method. In this technique the compounds are subject to photodissociation induced by UV light of a tunable laser and the resulting Cr atom is ionized by the resonant MPI with visible light of another tunable laser. In this method the dissociation proceeds under a low-intensity photon field of high-energy UV photons and the ionization is merely used as a means of sensitive detection of the resulting neutral Cr atom. The separation of the MPD from the MPI allows us to use a low-flux photon field for the photodissociation, so that a rate equation model of the overall process is applicable. On the basis of this advantage in the present method, we obtain the appearance energy of the Cr atom generated by the complete removal of all ligands from the compound.

In this work we investigate the dissociation of the following two compounds; tris(acetylacetonato)chromium(III) ($\text{Cr}^{\text{III}}(\text{acac})_3$) and hexacarbonylchromium(0) ($\text{Cr}^0(\text{CO})_6$), which are of basic importance in inorganic and organometallic chemistry [24].



In those two compounds, characteristics of the metal–ligand bonds are quite different from each other, as predicted by the molecular orbital theory of coordination compounds [25]. The substantial difference in the d-electron configuration is revealed by their absorption spectra; d–d transitions of the $\text{Cr}^{\text{III}}(\text{d}^3)$ complex occur in the visible region [26] while no visible transition is known in the $\text{Cr}^0(\text{d}^6)$ [27] complex. Characteristic mechanisms for the Cr atom generation are expected in

each system because of the difference in bonding nature. We have found the characteristic mass spectra representing the difference in dissociation process. The dissociation mechanisms in both systems are discussed on the basis of the observed results.

2. Experimental

In photodissociation studies of $\text{Cr}(\text{CO})_6$ in the ordinary gas phase, it has been reported that rate constants of bimolecular reactions between the resulting fragments and the residual vapor of the ligand (CO) are quite large [22,23]. In order to avoid the collisional effects, the present MPD/MPI experiment is thoroughly done in supersonic free jets of $\text{Cr}(\text{acac})_3$ or $\text{Cr}(\text{CO})_6$ vapor seeded in He carrier gas. A pulsed nozzle with an orifice of 0.8 mm in diameter was used to generate the free jet [28]. A heat-stable pulsed nozzle was made by replacing non-heat-resistant parts of a commercially available fuel injector with heat-proof materials. A solenoid was prepared by winding polyimide-coated copper wire (Thermotight C-7, 0.3 mm diameter, Showa Densen Denran Co.) on a core of machinable ceramics (Macore, Corning Co.). Heat-resistant O-rings (Kalrez, Dupont Co.) were also used for gas seals between the parts. The solenoid and an ordinary plunger unit were reassembled and put in a metal case of the injector. The whole nozzle unit was mounted into a stainless-steel housing with a heater. The crystalline powder of $\text{Cr}(\text{acac})_3$ or $\text{Cr}(\text{CO})_6$ was also put into the housing which was heated at about 180°C to obtain enough vapor pressure from the compound. The temperature was monitored by a calibrated platinum sensor mounted on the housing. The gaseous mixture of the compound and He at 3 atm was expanded into a vacuum chamber through the heated pulsed nozzle. The vacuum chamber and evacuation systems were the same as those described in detail elsewhere [29]. Briefly, the main chamber where the free jet was produced was evacuated by a turbomolecular pump system down to 5×10^{-5} Torr under 10 Hz operation of the pulsed nozzle. A subchamber which was equipped with a detection system for photoionized

species was also evacuated by a small turbo-molecular pump system down to 1×10^{-5} Torr.

The UV light used for the MPD was generated by a mixing-after-doubling system of the Nd:YAG laser pumped dye laser (Quantel Int. YG 581-10 + TDL50). Visible light from the dye laser was frequency doubled by a SHG crystal (KDP) and the resulting output was mixed with 1064 nm of the Nd:YAG laser by another KDP crystal. The UV light beams of 247–241 and 258–253 nm were obtained by using DCM and pridine-1 dye solutions, respectively. Light beams other than the UV light were removed by a beam separator having four Pellin–Broca prisms which were properly placed in order to avoid a beam walk off of the UV light during the wavelength scan of the dye laser. For the MPI the visible light of a N₂ laser pumped dye laser (Molelectron UV-24 + DL-14) was used. Two lasers were synchronously triggered by electric pulses from a digital delayed pulse generator, so that the visible light was delayed by about 100 ns with respect to the UV light pulse of about 14 ns in full width. The UV light beam was focused by a lens with a focal length of 25 cm and crossed the free jet 20 mm downstream from the nozzle. The visible light beam was also introduced into the chamber from the opposite direction of the UV light and coaxially focused by a lens with a focal length of 20 cm into the region where the free jet and the UV light beam crossed. In order to avoid simultaneous dissociation–ionization due to multiphoton excitation by each of the two laser beams alone, power densities of the two beams in the free jet region were adequately adjusted by changing their focuses. The laser power of the UV light measured at a point in front of the focusing lens was about $500 \mu\text{J}/0.5 \text{ cm}^2$ for Cr(acac)₃ and about $10 \mu\text{J}/0.5 \text{ cm}^2$ for Cr(CO)₆. The visible light of about $500 \mu\text{J}/0.2 \text{ cm}^2$ was used for the ionization of both compounds.

The fragments generated by the photodissociation with the UV light were successively ionized by the visible light and the resulting fragment ions were repelled from the crossing region by a positively charged plate to an entrance hole in the subchamber. The electric field strength between the plate and the grounded entrance hole was

about 15 V/cm. The ionic species were separated by a quadrupole mass filter (Extranuclear, 4-270-9) and detected by a channel electron multiplier. The ion current was amplified by a current amplifier and averaged by a box car integrator.

3. Results

3.1. Cr(acac)₃

3.1.1. One-color MPI spectrum

Fig. 1 shows a part of the MPI spectrum of Cr(acac)₃ obtained by the excitation with the visible light of 560–540 nm. The sharp lines are due to the two-photon resonant MPI of Cr atom which is generated by the MPD of Cr(acac)₃ with the same visible light. The index of the laser power dependence of the ion yield at the laser wavelength of 541.92 nm is found to be 6.4 ± 0.5 , showing that more than six photons are used for the one-color MPD/MPI spectrum. Since the ionization energy [30] of Cr is 54565 cm^{-1} , the ionization requires three photons in this wavelength region. Thus, more than three photons may be used for the dissociation to the Cr atom in the one-color MPD/MPI of the compound.

The transition energies of the two-photon resonances are listed in table 1, together with their assignments based on the atomic energy table [30]. The following two-photon transitions occur under the *LS* coupling selection rules; $\Delta L = 0, \pm 2$, $\Delta J = 0, \pm 1, \pm 2$ and $\Delta S = 0$. The most intense line is due to the transition from the ground state $a^7\text{S}_3$ to the excited state $e^7\text{S}_3$. Other lines are transitions from the low-lying excited states of $a^5\text{S}_2$ and $a^5\text{D}_{J''}$ ($J'' = 0-4$) to the higher excited state of $e^5\text{D}_{J'}$ ($J' = 0-4$). The multiplet structures are due to transitions with different ΔJ . The transitions observed in this spectral region involve three low-lying atomic states of Cr including the ground state; the levels of $a^5\text{S}_2$ and $a^5\text{D}_J$ ($J = 0-4$) [30] lie between 7593.16 and 8307.57 cm^{-1} relative to the ground state $a^7\text{S}_3$. Therefore, it is convenient to use these resonance lines in detecting the low-lying atomic states generated after the MPD of Cr coordination compounds.

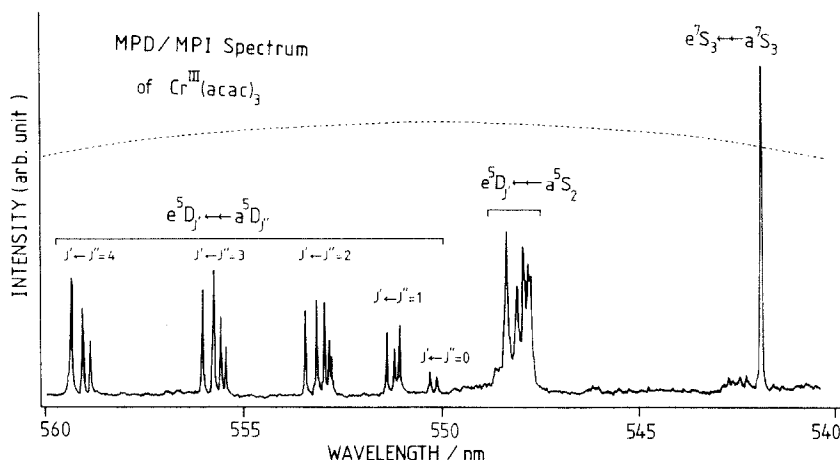


Fig. 1. One-color MPD/MPI spectrum of jet-cooled $\text{Cr}(\text{acac})_3$ obtained by monitoring the Cr^+ ion current. The sharp peaks are due to the two-photon resonances of Cr atom and their assignments are given. The dotted line represents the laser power spectrum of coumarin 540 A.

Under an experimental condition with tightly focused visible light of 580–400 nm we also observed the one-color MPD/MPI spectrum of

$\text{Cr}(\text{acac})_3$ in a larger spectral region than that described above. Laser wavelengths of the observed lines in the spectrum were essentially the same as those reported in the MPI spectrum of $\text{Cr}(\text{CO})_6$, given by Gerrity et al. [11].

Table 1
Resonance lines observed in the MPD/MPI spectrum of $\text{Cr}(\text{acac})_3$

Laser wavelength (nm)	Two-photon energy (cm^{-1})	Assignment (ref. [30])
541.92	36896	$e^7S_3 \leftarrow a^7S_3$
547.80	36499	$e^5D_0 \leftarrow a^5S_2$
547.86	36495	$e^5D_1 \leftarrow a^5S_2$
547.96	36489	$e^5D_2 \leftarrow a^5S_2$
548.16	36475	$e^5D_3 \leftarrow a^5S_2$
548.40	36459	$e^5D_4 \leftarrow a^5S_2$
550.16	36342	$e^5D_0 \leftarrow a^5D_0$
550.21	36339	$e^5D_1 \leftarrow a^5D_0$
550.34	36331	$e^5D_2 \leftarrow a^5D_0$
551.14	36279	$e^5D_1 \leftarrow a^5D_1$
551.26	36271	$e^5D_2 \leftarrow a^5D_1$
551.44	36259	$e^5D_3 \leftarrow a^5D_1$
552.87	36165	$e^5D_0 \leftarrow a^5D_2$
552.91	36162	$e^5D_1 \leftarrow a^5D_2$
553.03	36154	$e^5D_2 \leftarrow a^5D_2$
553.23	36141	$e^5D_3 \leftarrow a^5D_2$
553.51	36123	$e^5D_4 \leftarrow a^5D_2$
555.53	35992	$e^5D_1 \leftarrow a^5D_3$
555.65	35984	$e^5D_2 \leftarrow a^5D_3$
555.81	35974	$e^5D_3 \leftarrow a^5D_3$
556.07	35956	$e^5D_4 \leftarrow a^5D_3$
558.90	35775	$e^5D_2 \leftarrow a^5D_4$
559.10	35762	$e^5D_3 \leftarrow a^5D_4$
559.34	35747	$e^5D_4 \leftarrow a^5D_4$

3.1.2. Two-color MPI spectrum

As described above, the spectral region shown in fig. 1 is quite useful in detecting the low-lying atomic states and the flatness of the laser power spectrum is also convenient to simplify the normalization of the MPI spectrum. For these reasons, the two-color MPD/MPI experiment is carried out in the spectral region of the visible light given in fig. 1. When the UV light is fixed at 240 nm for the MPD and the laser wavelength of the visible light is scanned, the MPI spectrum of Cr is also obtained. The two-color MPD/MPI spectrum of $\text{Cr}(\text{acac})_3$ obtained in this way is shown in fig. 2a. Relative intensities of the three transitions are given in table 2 below.

In this experiment, we paid much attention to avoiding unwanted processes; the power density of the visible light is so reduced that the ion current is not observed in absence of the UV light. The mixed excitation processes due to the UV and visible light pulses are also removed by the temporal delay between the two light pulses. In spite of the reduction of the laser power a weak back-

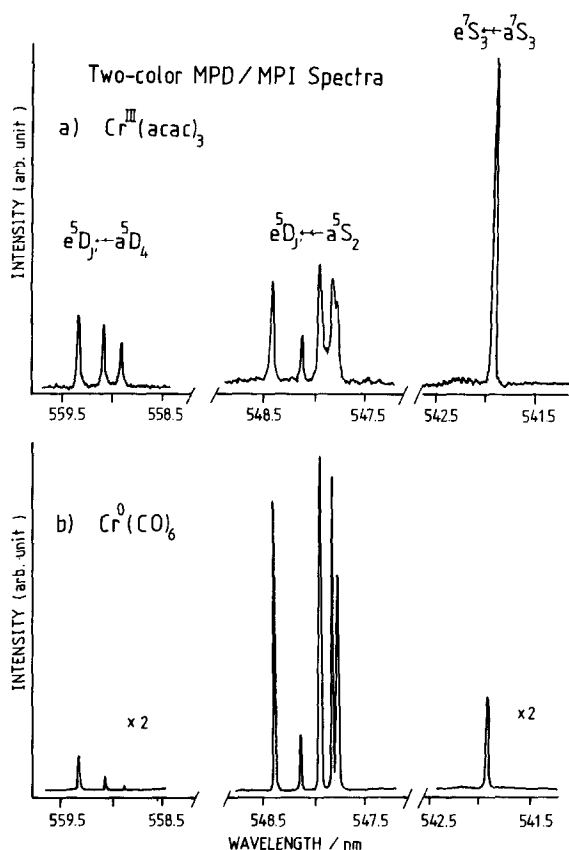


Fig. 2. Two-color MPD/MPI spectra of jet-cooled (a) $\text{Cr}(\text{acac})_3$ and (b) $\text{Cr}(\text{CO})_6$. Three spectral regions for the transitions of $e^5D_{j'} \leftarrow a^5S_4$, $e^5D_{j'} \leftarrow a^5D_{j''}$ and $e^7S_3 \leftarrow a^7S_3$ are given. The UV light for the Cr generation is fixed at 240 nm for $\text{Cr}(\text{acac})_3$ and at 242 nm for $\text{Cr}(\text{CO})_6$.

ground is observed and the line shapes of the atomic resonances are rather broad, showing the power broadening in the MPI process.

We note that transitions starting from much higher lying excited states of Cr than the a^5D state are not found in the two-color MPD/MPI spectrum. If the MPD prepares the a^5G_4 state, for example, the $g^5D_4 \leftarrow a^5G_4$ transition should appear at 576.8 nm. We do not find such a resonance line in the spectral region of 570–580 nm. This indicates that the present MPD prepares only the atomic states lying below the a^5D_4 state.

3.1.3. Threshold of the Cr generation

The yield spectrum of the Cr atom generation is obtained as a function of the laser wavelength

of the UV light. Fig. 3 shows the yield spectrum of the Cr atom originating from $\text{Cr}(\text{acac})_3$. In this spectrum, the laser wavelength of the visible light is fixed at the resonance line (541.92 nm) of the $e^7S_3 \leftarrow a^7S_3$ transition and the UV light is scanned for the dissociation. The yield increases in going to the energy region higher than the threshold at 254.8 ± 0.3 nm. As seen from fig. 3, however, the yield is not zero in the region lower than the threshold. The non-zero yield in the low-energy region suggests that the Cr atom is not generated by the one-photon dissociation process of the UV light but is produced by the multiphoton dissociation process.

In order to find the multiphoton energy for the Cr atom generation, the laser power dependences of the yield with respect to the UV light intensity are observed. Fig. 4 shows the power dependences of the yield for the UV photon energies above and below the threshold. The index of the power dependence is found to be 1.8 ± 0.2 with the UV

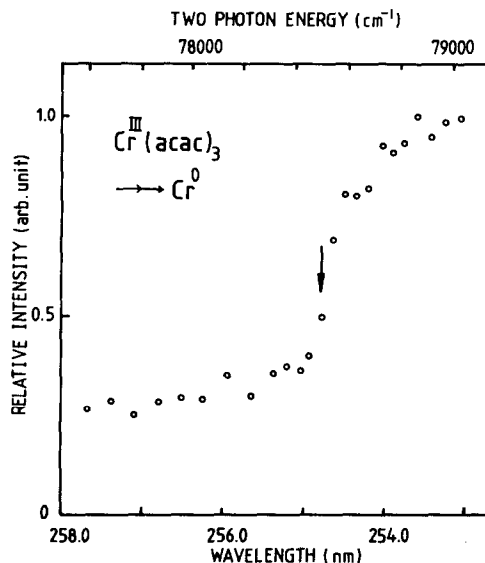


Fig. 3. The yield spectrum of the Cr atom generation obtained from the photodissociation of $\text{Cr}(\text{acac})_3$ by the UV light excitation. The Cr atom yield is monitored by the two-photon resonant MPI due to the $e^7S \leftarrow a^7S$ transition with the visible light fixed at 541.92 nm. The yield is normalized with respect to the laser power spectrum of the UV light. The threshold found at 254.8 ± 0.3 nm is due to the onset of the two-photon dissociation of $\text{Cr}(\text{acac})_3$, so that the two-photon energy scale is given on the top.

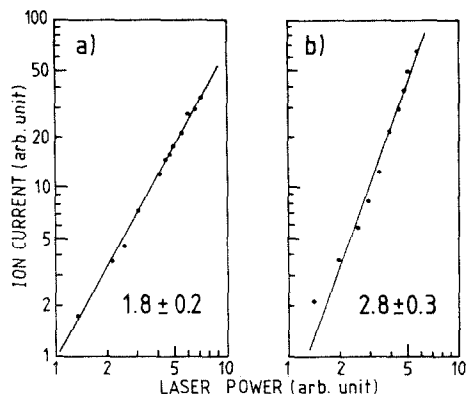


Fig. 4. Laser power dependences of the Cr atom generation from $\text{Cr}(\text{acac})_3$. The relative intensity of the Cr^+ ion current is measured by changing the intensity of the UV light at (a) 254.3 nm and at (b) 279.4 nm. In both dependences, the Cr atom yield is monitored by the two-photon resonant MPI with the visible light fixed at 541.92 nm. The indices of the power dependence are also given.

photon energy higher than the threshold, showing that the two-photon process is responsible for the dissociation. The result indicates that the threshold is due to the onset of the two-photon dissociation. The appearance energy of the Cr atom in the ground state a $^7\text{S}_3$ is therefore found to be $78500 \pm 100 \text{ cm}^{-1}$. When the $e^5\text{D}_2 \leftarrow a^5\text{S}_2$ and $e^5\text{D}_4 \leftarrow a^5\text{D}_4$ transitions are monitored, the thresholds for the generation of the excited state of Cr atom are also obtained. The threshold energies for the excited states are found to be the same as that obtained for the ground state. This indicates that the two-photon energy larger than the threshold at 78500 cm^{-1} produces the atomic fragments not only in the ground state but also in the excited states.

The weak background of the yield spectrum found in the energy region lower than the threshold is due to three-photon processes in the Cr atom generation. This is confirmed by the laser power dependence of the yield which exhibits the index of 2.8 ± 0.3 with the UV photon energy lower than the threshold as given in fig. 4b.

3.1.4. Two-color MPD/MPI mass spectrum

Fig. 5 shows the mass spectrum obtained by the MPD/MPI of $\text{Cr}(\text{acac})_3$. In the two-color MPD/MPI the Cr^+ ion ($M = 52 \text{ amu}$) is the only

species observed and neither $\text{Cr}(\text{acac})_3^+$ ion nor any other fragment ion is observed. In this spectrum the intensities of both UV and visible lights are so reduced that no ionic species is generated by the excitation with either light alone. This fact indicates that the Cr^+ ion does not originate from the $\text{Cr}(\text{acac})_3^+$ ion produced by the MPI, but is due to the ionization of the neutral Cr atom generated by the dissociation.

In the mass spectrum obtained by the excitation with the tight-focused UV light the CrO^+ fragment ion ($M = 68 \text{ amu}$) appears as intense as about one fifth of the Cr^+ peak. A similar mass spectrum after the MPI of $\text{Cr}(\text{acac})_3$ has been reported by Morris and Jonston [31], who studied the fragmentation of the metal β -diketonates using the fourth harmonic of Nd:YAG laser at 266 nm.

3.2. $\text{Cr}(\text{CO})_6$

The two-color MPD/MPI spectrum of $\text{Cr}(\text{CO})_6$ is shown in fig. 2b, where the UV light for the dissociation is fixed at 242.0 nm. These lines are also due to the same resonances of Cr as those described above in the section concerning $\text{Cr}(\text{acac})_3$. Relative intensities of these lines in fig. 2b are, however, quite different from those shown in fig. 2a. A comparison of the relative intensities of the observed lines for $\text{Cr}(\text{CO})_6$ with those for $\text{Cr}(\text{acac})_3$ is seen in table 2. In fig. 2, the most intense peak due to the $e^5\text{D}_2 \leftarrow a^5\text{S}_2$ transition for $\text{Cr}(\text{CO})_6$ is seven times stronger than the peak

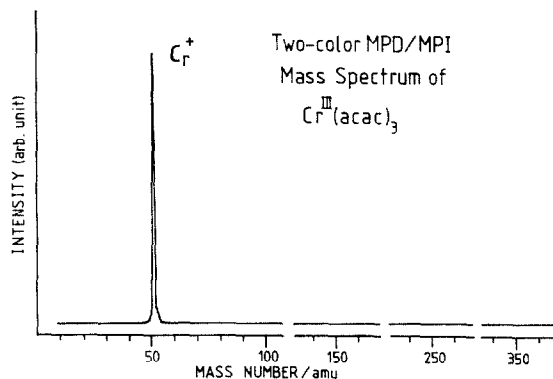


Fig. 5. Mass spectrum obtained by the two-color MPD/MPI of $\text{Cr}(\text{acac})_3$. The UV light is fixed at 254.3 nm and the visible light at 541.92 nm.

Table 2
Relative intensities of the atomic transitions in the two-color MPD/MPI spectra of $\text{Cr}(\text{acac})_3$ and $\text{Cr}(\text{CO})_6$

Transitions ^{a)}	$\text{Cr}(\text{acac})_3$	$\text{Cr}(\text{CO})_6$
$e^7S_3 \leftarrow a^7S_3$	1.0	1.0
$e^5D_2 \leftarrow a^5S_2$	0.35	7.40
$e^5D_4 \leftarrow a^5D_4$	0.22	0.41

^{a)} Transitions with $\Delta J = 0$ are used.

due to the $e^7S_3 \leftarrow a^7S_3$ transition which is the most intense line for $\text{Cr}(\text{acac})_3$. This result shows that the atomic state of a 5S_2 is well populated after the photodissociation of $\text{Cr}(\text{CO})_6$. The observed differences in the relative intensity must be associated with the atomic state population of the resulting Cr atom, showing that the dissociation process in $\text{Cr}(\text{CO})_6$ is different from that in $\text{Cr}(\text{acac})_3$. However, it is difficult to estimate the atomic state population from the observed intensities because of unknown cross sections of the two-photon resonance transitions.

Fig. 6 shows the yield spectrum of the a^5S_2 state of Cr generated from $\text{Cr}(\text{CO})_6$, where the visible light is fixed at 547.96 nm and the laser

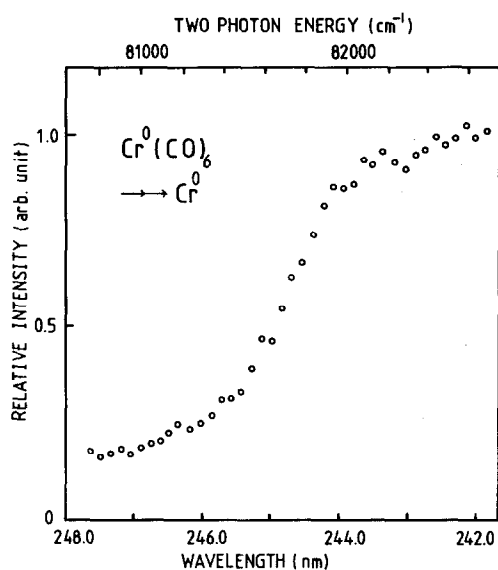


Fig. 6. The yield spectrum of the Cr atom generation obtained from the photodissociation of $\text{Cr}(\text{CO})_6$ by the UV light excitation. The Cr atom yield is monitored by the two-photon resonance MPI due to the $e^5D_3 \leftarrow a^5S_2$ transition with the visible light fixed at 547.96 nm.

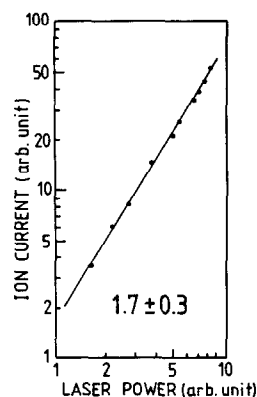


Fig. 7. Laser power dependence of the Cr atom generation from $\text{Cr}(\text{CO})_6$. The Cr^+ ion current intensity is measured by changing the intensity of the UV light at 242.0 nm. The Cr atom yield is monitored by the two-photon resonant MPI with the visible light fixed at 547.96 nm. The index of the power dependence is found to be 1.7 ± 0.3 .

wavelength of the UV light is scanned for the dissociation. The yield of the Cr atom increases gradually in going to the shorter-wavelength region with only a vague onset at about 246.3 nm. The laser power dependence of the yield is given in fig. 7 and the index of the dependence is found to be 1.7 ± 0.3 for the UV light at 242.0 nm. Therefore, the Cr atom from $\text{Cr}(\text{CO})_6$ is efficiently generated by the two-photon dissociation of the UV light and its threshold is located at about $81200 \pm 500 \text{ cm}^{-1}$. The threshold energy obtained for the generation of the ground state a^7S_3 is found to be the same as that obtained for the a^5S_2 state given above.

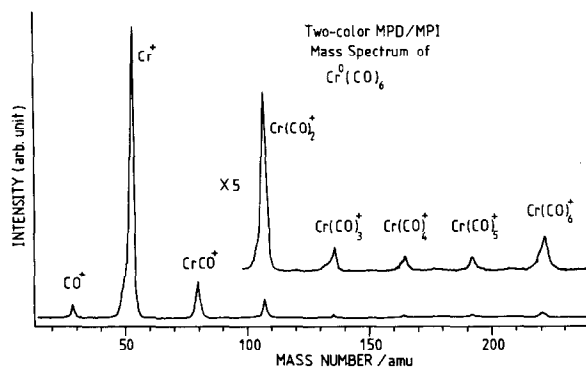


Fig. 8. Mass spectrum obtained by the two-color MPD/MPI of $\text{Cr}(\text{CO})_6$. The UV light is fixed at 242.0 nm, the visible light at 547.96 nm.

Fig. 8 shows the mass spectrum obtained by two-color MPD/MPI. Peaks of ionic species other than the CO^+ ion are found to be in a sequence with a mass interval of $M = 28$ amu from the intense Cr^+ peak ($M = 52$ amu) so that they are easily assigned to $\text{Cr}(\text{CO})_n^+$ ($n = 0-6$). We emphasize again that no ionic species is found by the excitation with the UV or visible light alone. The laser power dependences and the ionization yield spectrum for the ionic species of $\text{Cr}(\text{CO})_n^+$ ($n = 1-6$) are not obtained because of their weakness. Although details of the generation process of these species are not found, the result suggests that the neutral fragments $\text{Cr}(\text{CO})_n$ ($n = 1-5$) as well as the Cr atom are produced by the excitation with the UV light. These neutral fragments are well known in the transient infrared spectroscopy with UV excimer laser photolysis of $\text{Cr}(\text{CO})_6$ done by Weitz and co-workers [1,16,19] and by Fletcher and Rosenfeld [14,15,18].

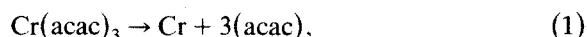
4. Discussion

4.1. $\text{Cr}(\text{acac})_3$

In the two-color MPD/MPI experiment, we have two important facts leading to the dissociation mechanism of $\text{Cr}(\text{acac})_3$; one is that the excited atomic states of Cr are produced as well as the ground state. The second is that the two-color MPD/MPI mass spectrum shows no photofragment other than the Cr^+ ion. First we discuss the dissociation energy in relation to the excited state generation. Secondly we shall concern ourselves with the results obtained from the mass spectrum, and finally discuss the energy scheme of the MPD/MPI process in $\text{Cr}(\text{acac})_3$.

As seen from the atomic energy table [30] there is a large energy gap between a $^5\text{D}_J$ and a $^5\text{G}_J$ states, that is, the third lowest state a $^5\text{D}_J$ is in $7750-8307\text{ cm}^{-1}$ whereas the fourth lowest state a $^5\text{G}_J$ is in $20517-20524\text{ cm}^{-1}$. No generation of a $^5\text{G}_J$ ($J = 2-6$) is found in the present condition and a $^5\text{D}_J$ ($J = 4$) located at 8307 cm^{-1} ($\approx 1.03\text{ eV}$) is the highest level produced. This indicates that the two-photon threshold energy observed at 78500 cm^{-1} ($\approx 9.73\text{ eV}$) for the Cr atom genera-

tion is large enough to produce all the atomic states located in energy not higher than a $^5\text{D}_J$ ($J = 4$). In the Cr atom generation, therefore, a part of the excitation energy is consumed by the excitation of these atomic states and is stored as internal energy (at least 1.03 eV) in the resulting Cr atom. The rest of the excitation energy is available for the dissociation of the metal-ligand bonds. As a result, the available energy of about 8.70 eV represents an upper limit of the dissociation energy for the neutral metal atom and ligands in their ground states,



where (acac) refers to the $\text{C}_5\text{H}_7\text{O}_2$ radical. This reaction may be called a homolytic dissociation with respect to the metal-ligand bonds. The enthalpy change in the homolytic dissociation of $\text{Cr}(\text{acac})_3$ in the gas phase was found to be 8.33 eV (192.02 kcal/mol) in the thermodynamical study of heats of combustion [32]. The upper limit of the dissociation energy is in accord with this thermodynamical value. By using the enthalpy change the energy diagram of the MPD/MPI process is obtained, as shown in fig. 9.

On the basis of the energy scheme, we discuss the dissociation mechanism of $\text{Cr}(\text{acac})_3$. As shown in fig. 9, the two-photon threshold of the dissociation is much higher than the ionization potential (IP) of $\text{Cr}(\text{acac})_3$, which is known to be 7.46 eV in the photoelectron spectrum [33]. By the absorption of two UV photons, therefore, $\text{Cr}(\text{acac})_3$ is excited to a dissociative state which is located at about 2.27 eV higher than the IP. Normally such a high energy excitation results in direct ionization or autoionization (vibrational and/or electronic), yielding the molecular ion. The fragmentation of the molecular ion may occur if the photoionization energy is large enough for the dissociation of the molecular ion. The molecular or fragment ions are then expected to be observed in the mass spectrum. In the case of $\text{Cr}(\text{acac})_3$, however, the two-color MPD/MPI mass spectrum indicates that the ionization followed by the fragmentation does not take place, but that the efficient generation of the neutral Cr atom does occur after the two-photon excitation. Thus the Cr atom generation must

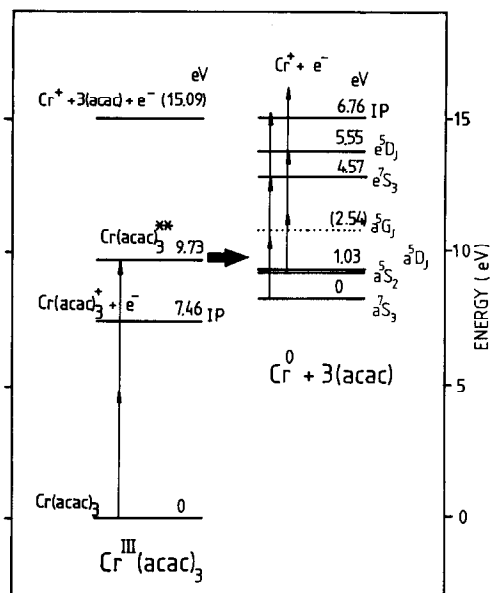
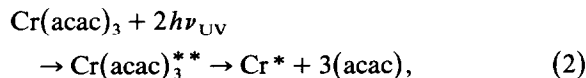


Fig. 9. Energy scheme for the MPD/MPI process in $\text{Cr}(\text{acac})_3$. The enthalpy change for $\text{Cr}(\text{acac})_3 \rightarrow \text{Cr} + 3(\text{acac})$ is taken to be 8.33 eV. The relative energies of the excited states and of the ionic states are indicated in eV.

occur within the neutral manifold of the highly excited $\text{Cr}(\text{acac})_3$. Neutral molecular states located above the IP are often called “super-excited states” [34]. Therefore the Cr atom originates from the super-excited state which interacts strongly with a dissociation continuum. Thus we conclude that the dissociation mechanism is the following:



where the double asterisk indicates the super-excited state and the single asterisk represents the ground or excited state of Cr.

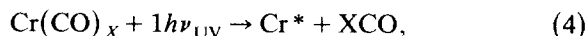
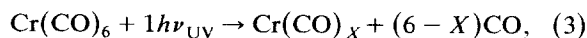
Though the super-excited state of the compound has not been reported, its characteristics obtained from the present result can be discussed with respect to the molecular symmetry and to the molecular orbital theory. The molecular symmetry of $\text{Cr}(\text{acac})_3$ is represented by the D_3 point group, the conformation of the methyl groups of the ligands being disregarded. The ground state is known to be 4A_2 . Since the two-photon transition operators belong to the A_1 and E representations,

the two-photon allowed states from the 4A_2 ground state should be 4A_2 and 4E , which should also be spin allowed. From the experimental point of view, on the other hand, it is suggested that all the metal–ligand bonds dissociate simultaneously from the super-excited state. Such a simultaneous dissociation of all ligands is expected only when the compound is excited to the dissociative excited state involving the totally symmetric $a_1(\sigma^*)$ MO of anti-bonding with respect to all metal–ligand bonds. Though the detailed MO calculation including σ^* orbitals of the compound is not known, a qualitative consideration of the MO energy levels predicts the presence of $a_1(\sigma^*)$ in the high-energy region. The 4s atomic orbital of Cr and the σ -type orbitals of the ligands create bonding MOs of $a_1(\sigma)$, $a_2(\sigma)$ and $2e(\sigma)$, and also an anti-bonding $a_1(\sigma^*)$ MO of the compound. They correspond to the well-known MOs of $a_{1g}(\sigma)$, $e_g(\sigma)$, $t_{1u}(\sigma)$ and $a_{1g}(\sigma^*)$ in the octahedral (O_h) symmetry [35]. On the other hand, 3d orbitals of Cr and the π -type orbitals of the ligands create $a_1(\pi)$, $a_2(\pi)$ and $e(\pi)$ MOs including the highest occupied MOs in the ground state. In this MO picture the excitation of one electron from an occupied MO of the e or a_1 symmetry to the anti-bonding $a_1(\sigma^*)$ MO leads to excited states of 4A_2 , 4E , 2A_1 and two 2E species. From the 4A_2 ground state, the transitions to the former two states are two-photon allowed and also spin allowed, whereas transitions to the latter three are spin forbidden. From the requirements for the two-photon allowedness and for the simultaneous dissociation, therefore, it is suggested that the super-excited state is either 4A_2 or 4E state, which originates from the excitation of one electron to the $a_1(\sigma^*)$ MO. This argument is not altered even when relatively stable π^* -type orbitals of the ligands are introduced in the MO picture. MOs involving the π^* orbitals do not interact with the $a_1(\sigma^*)$ MO because of the different symmetry in the D_3 group.

4.2. $\text{Cr}(\text{CO})_6$

Many studies of the photodissociation of $\text{Cr}(\text{CO})_6$ have been done and were thoroughly summarized in a recent review article given by Weitz [1]. By using the transient infrared spec-

troscopy of the carbonyl compounds, the production of the coordinatively unsaturated photofragments has recently been investigated. On the other hand, the one-color MPD/MPI spectroscopic studies did not succeed so far in detecting the photofragments other than the Cr^+ ion, because the extensive photolysis results in the complete ejection of all the ligands. Fisanick et al. observed no photofragments except for the Cr^+ ion [12]. In this respect, the mass spectrum obtained by the two-color MPD/MPI (fig. 8) provides evidence for the existence of the coordinatively unsaturated photofragments. The presence of the photofragments other than the Cr atom suggests that the sequential dissociation of the CO ligands is important in the Cr atom generation after the UV photolysis of $\text{Cr}(\text{CO})_6$. Therefore, the two-photon dissociation proceeds in the following ways:

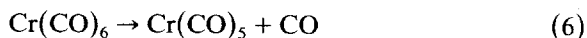


where $1 \leq X \leq 5$, and where the resulting Cr atom is either in the ground or excited state as represented by an asterisk. The threshold for the Cr atom generation is then determined by either reaction with a larger dissociation energy in the above two processes.

Since the threshold photon energy $h\nu_{\text{UV}}$ is found to be 5.05 eV, qualitative energetics of the dissociation can be obtained by using heats of formation of known reactions in the gas phase. The enthalpy change of the reaction.



is 6.51 eV ($\Delta H = 150 \pm 0.6$ kcal/mol) [36], and the dissociation energy of a single CO ligand in the reaction



has been reported to be 1.61 eV (37 kcal/mol) [37]. The energy difference (4.90 eV) between the processes (5) and (6) represents a lower limit of the decomposition energy of $\text{Cr}(\text{CO})_5$ into Cr and 5CO under assumption of no entropy change. Since $h\nu_{\text{UV}}$ of 5.05 eV exceeds the decomposition energy, it seems that $\text{Cr}(\text{CO})_5$ is energetically acceptable in processes (3) and (4), as far as the

ground state Cr atom is produced. However, the generation of the excited state of Cr atom in (4) requires an extra energy of about 1.03 eV in addition to the lower limit of the decomposition energy. Thus the energy leading to the dissociation into Cr^* and 5CO is not obtainable from $h\nu_{\text{UV}} = 5.05$ eV. Although no evidence specifying X in (3) and (4) is obtained in the present experiment, it has been known that the photofragment $\text{Cr}(\text{CO})_4$ is efficiently produced in the KrF laser photolysis of $\text{Cr}(\text{CO})_6$ [18–22]. The photon energy $h\nu_{\text{UV}}$ of 5.05 eV is very close to that of the KrF laser (248 nm, 5.0 eV), so that we may expect that the similar dissociation yielding the $\text{Cr}(\text{CO})_4$ fragment is effective in the processes (3) and (4). For the above reasons, we conclude that the threshold of the two-photon dissociation process in $\text{Cr}(\text{CO})_6$ producing the Cr atom is due to the one-photon threshold for the photodissociation of the photofragment $\text{Cr}(\text{CO})_4$.

5. Conclusions

Photodissociation processes of jet-cooled $\text{Cr}^{\text{III}}(\text{acac})_3$ and $\text{Cr}^0(\text{CO})_6$ have been investigated by using the two-color MPD/MPI method. The following conclusions have been obtained:

(i) Two-photon dissociation of $\text{Cr}(\text{acac})_3$ yielding the neutral Cr atom is found, and the threshold energy of the Cr atom generation is about 78500 cm^{-1} (9.73 eV).

(ii) The dissociation takes place from the neutral excited state lying above the ionization potential of $\text{Cr}(\text{acac})_3$, i.e. from the super-excited state.

(iii) The direct mechanism for the homolytic dissociation of $\text{Cr}(\text{acac})_3$ is proposed.

(iv) The threshold energy of the Cr atom generation in the two-photon photolysis of $\text{Cr}(\text{CO})_6$ is obtained.

(v) The sequential dissociation mechanism in the photolysis of $\text{Cr}(\text{CO})_6$ is confirmed by the two-color photoionized mass spectrum.

(vi) The observed threshold energy for the Cr atom generation from $\text{Cr}(\text{CO})_6$ is presumed to be due to the one-photon threshold for the dissociation of the photofragment(s).

Finally, we emphasize that the separation of the dissociation process from the ionization process in the two-color MPD/MPI method allows us to investigate the photodissociation of the metal–ligand compounds without taking into account the higher order interactions between compounds and a high intensity laser field, which are often encountered in the one-color MPD/MPI method.

Acknowledgement

We are grateful to Professor Mitsuo Ito for many stimulating discussions. This work was supported by a Grant-in-Aid from the Ministry of Education (No. 63540363).

References

- [1] E. Weitz, *J. Phys. Chem.* 91 (1987) 3945, and references therein.
- [2] A.B. Callear and R.J. Oldman, *Nature* 210 (1966) 730.
- [3] A.B. Callear and R.J. Oldman, *Trans. Faraday Soc.* 63 (1967) 2888.
- [4] Z. Karny, R. Naaman and R.N. Zare, *Chem. Phys. Letters* 59 (1978) 33.
- [5] R.L. Whetten, K.-J. Fu and E.R. Grant, *J. Chem. Phys.* 79 (1983) 4899.
- [6] S. Leutwyler, U. Even and J. Jortner, *Chem. Phys.* 58 (1981) 409.
- [7] S. Leutwyler, U. Even and J. Jortner, *J. Phys. Chem.* 85 (1981) 3026.
- [8] Y. Nagano, Y. Achiba and K. Kimura, *J. Phys. Chem.* 90 (1986) 1288.
- [9] Y. Nagano, Y. Achiba and K. Kimura, *J. Chem. Phys.* 84 (1986) 1063.
- [10] M.A. Duncan, T.G. Dietz and R.E. Smalley, *Chem. Phys.* 44 (1979) 415.
- [11] P.D. Gerrity, L.T. Rothberg and V. Vaida, *Chem. Phys. Letters* 74 (1980) 1.
- [12] G.J. Fisanick, A. Gedanken, T.S. Eichelberger IV, A.N. Kuebler and M.B. Robin, *J. Chem. Phys.* 75 (1981) 5215.
- [13] J.A. Welch, K.S. Peters and V. Vaida, *J. Phys. Chem.* 86 (1982) 1941.
- [14] D.P. Gerrity, L.J. Rothberg and V. Vaida, *J. Phys. Chem.* 87 (1983) 2222.
- [15] J.M. Hossenlopp, B. Samoriski, D. Rooney and J. Chaiken, *J. Chem. Phys.* 85 (1986) 3331.
- [16] G.W. Tyndall and R.L. Jackson, *J. Am. Chem. Soc.* 109 (1987) 582.
- [17] W. Tumas, B. Gitlin, A.M. Rosan and J.T. Yardley, *J. Am. Chem. Soc.* 104 (1982) 55.
- [18] T.R. Fletcher and R.N. Rosenfeld, *J. Am. Chem. Soc.* 105 (1983) 6358.
- [19] T.R. Fletcher and R.N. Rosenfeld, *J. Am. Chem. Soc.* 107 (1985) 2203.
- [20] T.A. Seder, S.P. Church, A.J. Ouderkerk and E. Weitz, *J. Am. Chem. Soc.* 107 (1985) 1432.
- [21] W.H. Brechenridge and G.M. Stewart, *J. Am. Chem. Soc.* 108 (1986) 364.
- [22] T.R. Fletcher and R.N. Rosenfeld, *J. Am. Chem. Soc.* 108 (1986) 1686.
- [23] T.A. Seder, S.P. Church and E. Weitz, *J. Am. Chem. Soc.* 108 (1986) 4721.
- [24] H. Kido and K. Saito, *J. Am. Chem. Soc.* 110 (1988) 3187.
- [25] G.L. Geoffroy and M.S. Wrighton, *Organometallic photochemistry* (Academic Press, New York, 1979).
- [26] R.L. Lintvedt, in: *Concepts of inorganic photochemistry*, eds. A.W. Adamson and P.D. Fleischauer, (Wiley, New York, 1974) ch. 7.
- [27] N.A. Beach and H.B. Gray, *J. Am. Chem. Soc.* 90 (1968) 5713.
- [28] N. Mikami, A. Hiraya, I. Fujiwara and M. Ito, *Chem. Phys. Letters* 74 (1980) 531.
- [29] N. Mikami, I. Suzuki and A. Okabe, *J. Phys. Chem.* 91 (1987) 5242.
- [30] C.E. Moore, *Atomic energy levels*, Vol. 2, NBS Circular 35 (Nat. Bur. Stds., Washington, 1971).
- [31] J.B. Morris and M.V. Johnston, *J. Phys. Chem.* 89 (1985) 5399.
- [32] M.M. Jones, B.J. Yow and W.R. May, *Inorg. Chem.* 1 (1962) 166.
- [33] S. Evans, A. Hamnett, A.F. Orchard and D.R. Lloyd, *Faraday Discussions Chem. Soc.* 54 (1972) 227.
- [34] J. Berkowitz, *Photoabsorption, photoionization, and photoelectron spectroscopy* (Academic Press, New York, 1979).
- [35] C.J. Ballhausen and H.B. Gray, *Molecular orbital theory* (Benjamin, New York, 1965).
- [36] G. Pilcher, M.J. Ware and D.A. Pittam, *J. Less-Common Metals* 42 (1975) 223.
- [37] K.E. Lewis, D.M. Golden and G.P. Smith, *J. Am. Chem. Soc.* 106 (1984) 3905.